Brillouin optical time-domain analysis sensor with pump pulse amplification

Juan José Mompó, Javier Urricelqui, and Alayn Loayssa*

Departamento de Ingeniería Eléctrica y Electrónica, Universidad Pública de Navarra
Campus de Arrosadía s/n, 31006, Pamplona, Spain

**alayn.loayssa@unavarra.es*

Abstract: We demonstrate a simple technique to provide conventional Brillouin optical time-domain analysis sensors with mitigation for pump pulse attenuation. The technique is based on operating the sensor in loss configuration so that energy is transferred from the probe wave to the pump pulse that becomes amplified as it counter-propagates with the probe wave. Furthermore, the optical frequency of the probe wave is modulated along the fiber so that the pump pulse experiences a flat total gain spectrum that equally amplifies all the spectral components of the pulse, hence, preventing distortion. This frequency modulation of the probe brings additional advantages because it provides increased tolerance to non-local effects and to spontaneous Brillouin scattering noise, so that a probe power above the Brillouin threshold of the fiber can be safely deployed, hence, increasing the signal-to-noise ratio of the measurement. The method is experimentally demonstrated in a 100-km fiber link, obtaining a measurement uncertainty of 1 MHz at the worst-contrast position.

OCIS codes: (290.5900) Scattering, stimulated Brillouin; (060.2370) Fiber optics sensors; (999.999) Brillouin optical time domain analysis; (999.999) Brillouin amplification.

References and links

1. M. Alem, M. A. Soto and L. Thévenaz, "Analytical model and experimental verification of the critical power for modulation instability in optical fibers," Opt. Express **23**(23), 29514–29532 (2015).
2. S. M. Foaleng, F. Rodríguez-Barrios, S. Martín-López, M. González-Herráez and L. Thévenaz, "Detrimental effect of self-phase modulation on the performance of Brillouin distributed fiber sensors," Opt. Lett. **36**(2), 97–99 (2011).
3. Y. Dong, L. Chen and X. Bao, "Extending the sensing range of Brillouin optical time-domain analysis combining frequency-division multiplexing and in-line EDFAs," J. Lightwave Technol. **30**(8), 1161–1167 (2012).
4. X. Angulo-Vinuesa, S. Martín-López, J. Nuño, P. Corredera, J. D. Ania-Castañon, L. Thévenaz and M. González-Herráez, "Raman-assisted Brillouin distributed temperature sensor over 100 km featuring 2 m resolution and 1.2°C uncertainty," J. Lightwave Technol. **30**(8), 1060–1065 (2012).
5. S. Le Floch, F. Sauser, M. Llera and E. Rochat, "Novel Brillouin optical time-domain analyzer for extreme sensing range using high power flat frequency coded pump pulses," J. Lightwave Technol. **33**(12), 2623–2637 (2015).
6. J. Urricelqui, M. Sagues and A. Loayssa, "Brillouin optical time-domain analysis sensor assisted by Brillouin distributed amplification of pump pulses," Opt. Express **23**(23), 30448–30458 (2015).
7. H. Q. Chang, X. H. Jia, X. L. Ji, C. Xu, L. Ao, H. Wu, Z. N. Wang and W.L. Zhang "DBA-based BOTDA using optical-comb pump and pulse coding with a single laser, " Photon. Technol. Lett. **28**(10), 1142-1145 (2016).
8. R. Ruiz-Lombera, J. Urricelqui, M. Sagues, J. Mirapeix, J. López-Higuera and A. Loayssa, "Overcoming nonlocal effects and Brillouin threshold limitations in Brillouin optical time-domain sensors," IEEE Photon. Journal, IEEE **7**(6), 1–9 (2015).
9. A. Zadok, A. Eyal and M. Tur, "Gigahertz-wide optically reconfigurable filters using stimulated Brillouin scattering," J. Lightwave Technol. **25**(8), 2168–2174 (2007).

#260529 Received 4 Mar 2016; revised 2 May 2016; accepted 4 May 2016; published 1 Jun 2016

10. X. Bao, J. Dhliwayo, N. Heron, D. Webb and D. Jackson, "Experimental and theoretical studies on a distributed temperature sensor based on Brillouin scattering," J. Lightwave Technol. **13**(7), 1340–1348 (1995).
11. M. van Deventer and A. Boot, "Polarization properties of stimulated Brillouin scattering in single-mode fibers," J. Lightwave Technol. **12**(4), 585–590 (1994).
12. G. Agrawal, "Nonlinear phase shift" in *Nonlinear Fiber Optics* (Academic, 2013), pp. 88–90.
13. W. Li, X. Bao, Y. Li and L. Chen, "Differential pulse-width pair BOTDA for high spatial resolution sensing," Opt. Express **16**(26), 21616–21625 (2008).
14. Y. Awaji, H. Furukawa, B. Puttnam, N. Wada, P. Chan and R. Man, "Burst-mode optical amplifier," *in Proceeding of Optical Fiber Communications*, (Optical Society of America, 2010), pp. 1–3.

1. Introduction

In the last years, Brillouin optical time-domain analysis (BOTDA) sensors have been used to monitor the integrity of structures such as oil and gas pipelines or to assess the temperature of the cable in high voltage transmission lines. These, and other applications, have a common need for distributed sensors that can monitor large distances.

However, the sensing range of BOTDA sensors is fundamentally limited by pump attenuation in the optical fiber, which makes the measured probe signal coming from Brillouin interaction at distant location along the fiber to be very small to be properly detected with the required signal-to-noise ratio (SNR). This problem can be compensated to some extend by increasing the pulse power. However, this is also limited because the use of large pump power leads to the onset of nonlinear effects such as modulation instability [1] or self-phase modulation (SPM) [2].

The obvious solution is to amplify the pulses along the fiber link to compensate their propagation attenuation. This has been demonstrated by the use of erbium-doped fiber amplifiers (EDFA) as pulse repeaters along the fiber length [3]. However, distant EDFAs need to be powered, whereas an all-passive sensing network is much more attractive. Another solution is to use distributed Raman amplification (DRA) by injecting a Raman pump in the sensing fiber [4]. However, this requires the use of very high power (of the order of Watts) in the fiber, which can become an eye-safety concern in the installation and operation of real systems. Moreover, using DRA, the relative intensity noise of the Raman pump laser can be translated to the detected signal, significantly degrading the measurement performance [4]. Another option to extend the measurement range is the use of coding [5].

We have recently introduced an alternative solution based on amplifying the pump pulses in the fiber using a distributed Brillouin amplifier (DBA) [6]. This technique is based on injecting in the fiber another laser source acting as DBA pump that amplifies the pulsed signal and does not increase the noise on the detected probe wave. Further work has been done using a DBA-BOTDA configuration with a single laser source and the use of coding [7]. In addition, we have been working lately on the compensation of the other two factors that limit the probe wave power and hence, the sensing range: non-local effects and Brillouin threshold of the fiber. In order to simultaneously compensate both factors, we have introduced a dual-probe-sideband BOTDA setup in which the optical frequency of the probe waves is modulated along the fiber [8].

In this work, we have built upon our previous contributions by introducing a simple modification to conventional BOTDA sensors that simultaneously provides compensation of pulse attenuation along the fiber and allows to increase the power of probe wave by mitigating non-local effects and the intensity noise induced when injecting a probe power larger than the Brillouin threshold of the fiber. The technique is based on operating the sensor in a loss configuration, so that energy is transferred from the probe wave to the pump pulse, and on modulating the optical frequency of the probe wave along the fiber.

#260529 Received 4 Mar 2016; revised 2 May 2016; accepted 4 May 2016; published 1 Jun 2016

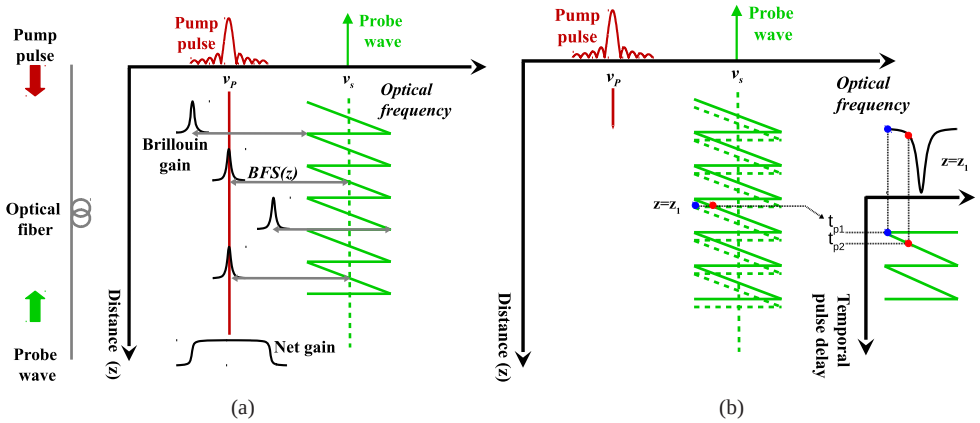

Fig. 1. (a) Spectra of the optical waves present in the optical fiber and (b) frequency scanning method based on the temporal delay between probe and pump waves.

2. Description of the technique

Figure 1(a) highlights the fundamentals of the technique in which two optical waves, probe wave and pump pulse, are used as in any conventional BOTDA sensor. As it is shown, the BOTDA sensor is set in a loss-based configuration so that the pump pulses generate a loss spectrum for the counter-propagating probe wave at every position along the fiber. Simultaneously, the probe wave also transfers energy to the pump as they interact along the fiber. The only modification to the conventional loss-based setup is that the probe wave optical frequency is modulated with a saw-tooth shape so that at every location of the fiber, as it is schematically depicted in Fig. 1(a), the Lorentzian gain spectrum experienced by the pulses is slightly offset in frequency. This makes the center optical frequency of the Brillouin gain spectra experienced by the pump pulses to vary along the fiber as it meets the optical-frequency-modulated probe wave front, so that the pulse experiences a broad total integrated gain spectrum. This net gain spectrum can be made to have a flat frequency response with a judicious choice of modulation shape, frequency and peak deviation [9]. Furthermore, the frequency modulation of the probe needs to be synchronized to the pulsed signal so that a sequence of pulses experience the same optical frequency of the probe wave at any given location.

In addition, the frequency modulation of the probe wave is also used to perform the frequency scan of the Brillouin spectra instead of using the conventional frequency swept. Figure 1(b) schematically depicts the method to scan the loss spectra at every location of the fiber simultaneously, which simply requires to change the temporal delay between the probe wave modulation and the pump pulse [8]. As it is shown in the figure, the modification of the delay between the frequency modulating signal and the pulses displaces the relative z-location of the saw-tooth because the pump pulse meets a given probe wavefront at a different time and position, which makes the probe wave at every location to experience a different detuning of the Brillouin spectrum. In order to scan the full Brillouin spectra, a total delay that equals the period of the saw-tooth wave is divided in as many delay steps as needed to have a spectral swept with the desired finesse (note that, for clarity, just two steps are shown in the figure). Therefore, after a total delay equivalent to the period of the saw-tooth, all frequencies within the peak-to-peak deviation of the frequency modulation have been scanned at all locations in the fiber simultaneously. Notice that there is no measurement time penalty in this setup compared to

#260529 Received 4 Mar 2016; revised 2 May 2016; accepted 4 May 2016; published 1 Jun 2016

a conventional frequency-swept BOTDA and hence, both systems require an identical number of measurements to characterize the full Brillouin spectrum for every position of the fiber.

The theoretical model for the interaction of the two waves depicted in Fig. 1(a) is based on the solution of the well-known steady-state coupled wave equations for the pump and probe optical intensities [10]. This gives the expression of the evolution of the pump pulse power along the fiber as:

$$P_P(z) = P_P(0)\exp\left[\int_0^z \frac{\eta(z) g_B(\Delta\nu)}{A_{eff}} P_S(L)\exp(-\alpha(L-z))\,dz\right]\exp(-\alpha z) \tag{1}$$

where $P_P(0)$ and $P_S(L)$ are the pump and probe powers injected in the fiber, respectively, L is the fiber length, A_{eff} is the effective area, α is the atenuation of the optical fiber and g_B is the local Brillouin gain coefficient, which depends on $\Delta\nu$, the local detuning of the pump pulse and probe wave frequencies from the center of the Lorentzian Brillouin spectrum, which is given by:

$$\Delta\nu(z) = \nu_P - \nu_S(z) + BFS(z) \tag{2}$$

with ν_P and ν_S, the optical frequencies of the pump and probe waves, respectively, and BFS the local Brillouin frequency shift. Notice that $\Delta\nu$ is made to vary along the fiber by the modulation of the optical frequency of the probe wave so that the total gain given by the exponential term containing the integral in Eq. (1) is as flat as possible, equally amplifying all the spectral components of the pulse. This model assumes pulses that are longer than the acoustic phonon lifetime (10 ns).

Finally, the $\eta(z)$ term in Eq. (1) is the mixing efficiency related to the relative state of polarization (SOP) of the pump and probe waves at a given location in the fiber [11]. It has been shown that in low-birefringence single-mode optical fibers, the total logarithmic gain experienced by the pulse in long fibers would vary between $1/3$ (for orthogonal counter-propagating signal) and $2/3$ (for parallel counter-propagating signals) of that obtained for ideal polarization maintaining fiber in which the SOP of the pump and probe wave remains identical along the fiber [11]. However, as it is discussed below, in this system we are not only concerned with the total integrated gain for the pulse, but also with the effects of the relative polarization of pump and probe have upon the Brillouin interaction experienced by the latter wave.

3. Experimental setup

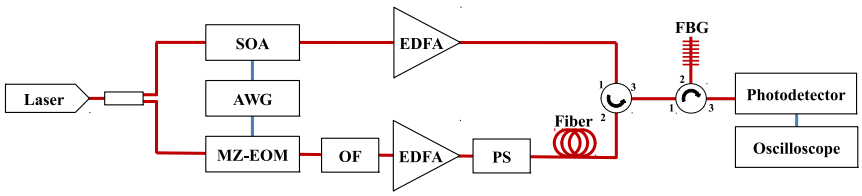

Fig. 2. Experimental setup for the BOTDA sensor based on frequency modulation of the probe wave.

Figure 2 schematically depicts the setup used to demonstrate our technique. We modify the conventional BOTDA by adding an arbitrary waveform generator (AWG) to frequency modulate the microwave signal applied to the Mach-Zehnder electro-optic modulator (MZ-EOM) used to generate the probe wave. This MZ-EOM is biased at minimum transmission in order to generate a double-sideband suppressed-carrier signal. The deployed

#260529 Received 4 Mar 2016; revised 2 May 2016; accepted 4 May 2016; published 1 Jun 2016

AWG has a sampling rate of 25 GSamples/s and a bandwidth of around 6 GHz, which is increased by the deployment of a frequency doubler. As a consequence, the bandwidth is large enough to generate the Brillouin frequency shift (around 10.8 GHz) necessary to stimulate the Brillouin scattering proces. This AWG provides a FM microwave signal whose instantaneous frequency varies around the average BFS already defined of the fiber following a saw-tooth shape with a period of 12.5 milliseconds and peak-to-peak frequency deviation of 200 MHz. A lower-cost alternative to the use of the AWG would be to deploy a microwave voltage control oscillator driven by a saw-tooth signal.

The frequency modulating signal is synchronized to the electrical pulse signal applied to a semiconductor optical amplifier (SOA) switch used to shape the pump pulse in the upper branch. This electrical pulse is generated on the same AWG than the FM signal. After the MZ-EOM, the lower-frequency sideband is filtered out by an optical filter (OF). Finally, the probe wave is boosted to 9 dBm using an EDFA and its polarization state is randomized using a polarization scrambler (PS) before been injected into 100-km of G.652 sensing fiber made with two spools of 50 km each. In the upper branch, the pulse is amplified in an EDFA to a peak power of 70 mW and launched into the fiber.

4. Experimental results

Figure 3 compares the distribution of the Brillouin spectra measured along the fiber with a dual-probe-sideband BOTDA [8] and for the new BOTDA with amplification of the pump pulse. For the dual-probe BOTDA, the amplitude of the Brillouin spectra decays exponentially due to the attenuation of the pump pulse as it propagates through the fiber. In contrast, in our system, the amplitude initially decays but starts to recover at a distance of around 30 km from the pump input, as it can be seen more clearly in the BOTDA trace in fig.4. At that distance the gain provided by the probe wave to the pump pulse starts to be significant. Considering that the gain experienced by the pump pulse does not increase the noise level in the measured response of the sensor [6], the increment of the detected amplitude along the fiber translates into an enhancement of the SNR. Notice that this is a BOTDA in loss configuration, but the amplitude of the traces have been inverted for clarity.

Figure 5 highlights the effects of polarization on the measured BOTDA signal. It is well-known that the relative polarization state of the pump and probe waves at each location of the fiber determines the mixing efficiency of the gain (or loss) experienced by the probe. This is given by the $\eta(z)$ factor discussed in section 2 that goes from $\eta(z) = 0$, for orthogonal polarization, to $\eta(z) = 1$, for identical polarization. Therefore, the common practice is to scramble the polarization of one of the two waves while performing the average of a number of acquisitions of the measurement, so that an average $\eta(z) = 1/2$ response is obtained. However, in our setup, the interplay of the polarization of pump and probe waves is more complex than in conventional BOTDA because the change of the relative polarization state of the two waves also influences the gain experienced by the pulse (Eq. 1) as it travels along the fiber. This gain, as it was discussed above (section 2), ranges from $2/3$ to $1/3$ of the maximum ideal value obtained for a fiber with no birefringence and identical SOP of pump and probe wave [11].

The two traces shown in Fig. 5 compare the measured BOTDA signal with the PS either in the upper branch of the setup after the EDFA, or in the lower branch. Notice that the polarization-induced noise with the PS in the upper branch is larger than when it is in the lower branch, particularly, at the final part of the fiber where the pulse is amplified. The reason for this is that when the scrambler is in the pump branch, the successive pump pulses arrive to a particular position, *z*, of the fiber with different polarization for each measurement realization. However, contrary to conventional BOTDA, the gain experience by successive pulses is going

#260529 Received 4 Mar 2016; revised 2 May 2016; accepted 4 May 2016; published 1 Jun 2016

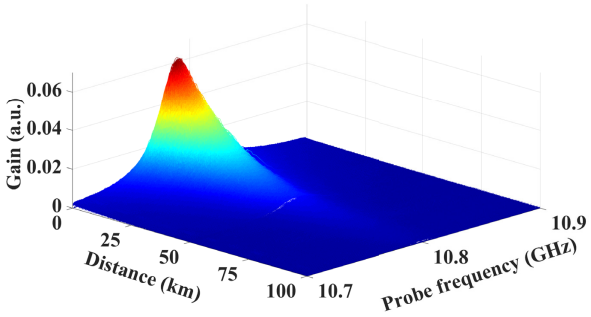

(a)

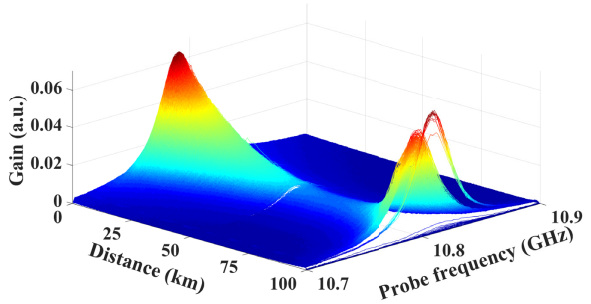

(b)

Fig. 3. Brillouin gain distribution measured with (a) dual-probe-sideband BOTDA sensor using frequency modulation of the probe wave and (b) novel BOTDA with pulse amplification. A pulse duration of 45 ns was deployed in both measurements.

to also change for each input SOP generated by the PS. Therefore, the Brillouin interaction (loss in this setup) experienced by the probe at that particular, z, does not average in general to a $\eta(z) = 1/2$ factor as in a conventional BOTDA. The average $\eta(z)$ depends on the particular SOP of the probe at that location and its relative orientation to the SOP of the pump pulse with maximum and minimum gain. In fact, it was observed that the averaged interaction at each particular location of the fiber changed over time due to the slow drift of the relative SOP of probe and pump pulse. This latter effect can severely degrade measurements due to amplitude drifts when the full Brillouin spectra is scanned. The problem with polarization just described can be solved by placing the PS in the probe branch because, in this case, during the course of averaged measurements, the successive pump pulses arrive at each particular location with an average gain after counter-propagating with the probe wave of aleatorized polarization. Then, as the measurement in Fig. 5 highlights, a stable averaged Brillouin interaction is experienced by the probe wave at each location.

Figure 6 introduces the details of the amplification of the pump pulses in the fiber. The pulses at the input of the fiber and at the output with and without gain are compared for pulses with 45-ns and 55-ns durations. The pulses are amplified by 19.6 dB, compensating the fiber link attenuation. Notice that the amplified pulse has its leading edge smoothed so that the rise time increases. However, the trailing edge maintains the original fall time previous to amplification. This behavior is explained by the fact that stimulated Brillouin scattering is a dynamic phenomena that depends on the interaction of a pump and Stokes waves via an

#260529
Received 4 Mar 2016; revised 2 May 2016; accepted 4 May 2016; published 1 Jun 2016

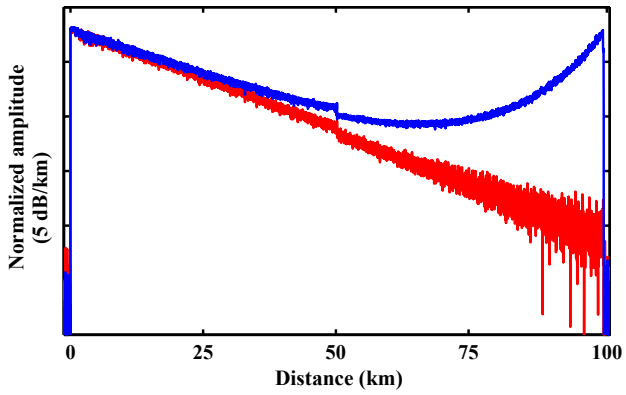

Fig. 4. Mesured traces of dual-probe-sideband BOTDA (red line) and BOTDA with pulse gain (blue line) using 45-ns pulse duration.

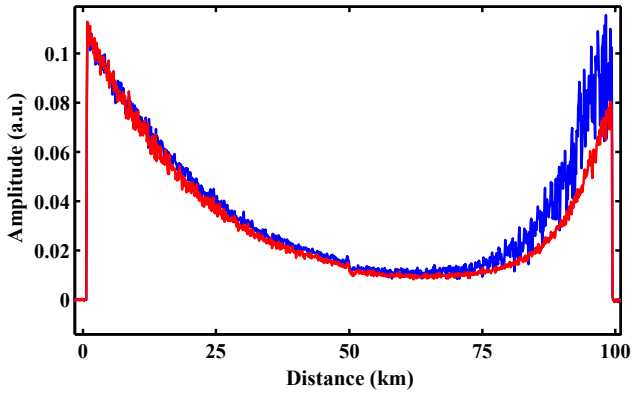

Fig. 5. BOTDA trace depicting the comparison of the measured polarization noise when the polarization scrambler is either used on the probe wave (red line) or on the pump pulse (blue line)

acoustic wave. The probe wave, which acts as pump wave in this interaction, is present at a certain location in the fiber and then, when the pump pulse (Stokes wave) arrives, an acoustic wave is created and the gain starts to gradually grow until it reaches an steady state (if the pulse is long enough) and, finally, the gain is abruptly cut-off as the pulse leaves.

This is an effect that distorts the pulse shape and that can lead to a BFS error induced by SPM, as we have previously observed [6]. SPM changes the instantaneous optical frequency of a pulse by [12]:

$$\Delta f(t) = -\frac{\gamma L_{eff}}{2\pi}\frac{dP(t)}{dt} \tag{3}$$

where γ is the nonlinear coefficient of the fiber, L_{eff} is the effective fiber length and P(t) is the temporal shape of the pulsed wave. Previous studies have reported on the influence of this instantaneous frequency shift in BOTDA sensors when using pulses that are symmetrical in the time domain and have relatively slow transitions [2]. In that case, SPM induces a symmetrical broadening of the pulse spectrum because Δf in the leading and trailing edges of the pulse have equal amplitude and opposite sign. Then, the broadening of the pulse spectrum leads to

#260529 Received 4 Mar 2016; revised 2 May 2016; accepted 4 May 2016; published 1 Jun 2016

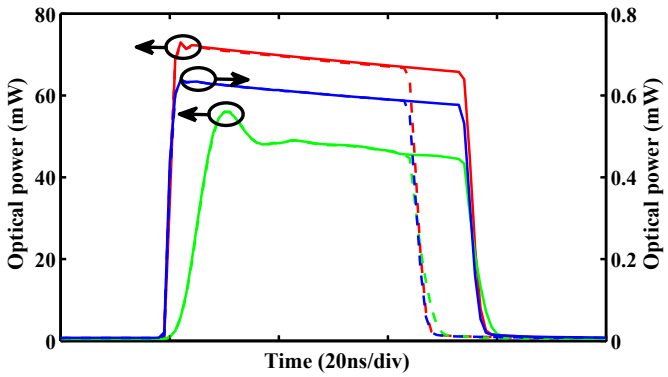

Fig. 6. Amplification of pump pulses with 45-ns (dashed line) and 55-ns (solid line) duration. Pulses are shown at the input of the fiber (red line), output of the fiber without gain (blue line) and amplified pulses (green line).

a broadening of the measured Brillouin spectrum linewidth. However, when an asymmetry in the time-domain shape of a pulse is introduced, like the rise-time smoothing induced by the Brillouin gain in this case, SPM induces an asymetrical broadening of the pulse spectrum that leads to an error in the measured BFS [6].

Nevertheless, in our BOTDA with gain, the BFS measurement error due to SPM can be avoided by deploying differential pulse-width pair (DPP) measurements [13], which subtract the response of two pulses with different durations, such as the ones depicted in Fig. 6. This eliminates the effect of the instantaneous optical frequency shift in the smoothed leading edge of the pulses. Moreover, the use of DPP also helps to solve another problem that is caused by the smoothing of the leading edge of the amplified pulse. This effect induces a change in the effective spatial resolution along the fiber as it can be observed in Fig. 6, in which the pulse at the output of the fiber becomes narrower compared to the pulse at the input of the fiber. However, DPP measurement provides a constant resolution independently of the gain of the pulse. This is due to the fact that the DPP technique involves the subtraction of the response to the common part of both pulses and the measurement of just the response to the differential part between both pulses. The differential part, as shown in Fig. 6, is identical for the pulses at the input and output of the fiber. Therefore, the DPP measurement provides a constant resolution of 1 meter (55 ns-45 ns=10ns$\sim$ 1m).

Figure 7 displays the measured BFS distribution in the fiber using DPP technique with two pulses of 45 and 55 ns. Two measurements were sequentially performed with the fiber inputs swapped so as to make sure that the BFS distribution is identical independently of which end is used to inject the probe and pump waves and hence that SPM or non-local effects are not introducing any significant errors. In order to avoid the influence of the temperature variations of the room, where the experiment was carried out, the last 140 m of the fiber link in which a different type of SMF with a slightly different BFS was kept at constant temperature using a climatic chamber. The detail of the BFS measured at this fiber section is shown in the inset of Fig. 7, where an almost identical BFS for both measurements can be observed. It can be also seen that the BFS in the rest of the fiber outside the climate chamber slightly varies between both measurements because of the temperature changes in the room. Notice that, in the temperature-controlled fiber length, in the there is a residual BFS difference of around 0.5 MHz for the measurement in both directions. This small difference is attributed to the effect of the EDFA

#260529 Received 4 Mar 2016; revised 2 May 2016; accepted 4 May 2016; published 1 Jun 2016

amplification on the pulse shape. As it can be seen in Fig. 6, the top of the pulses are not completely flat, but have a small slope due to transient effects in the EDFA. This slope, according to Eq. 3, leads to a small positive shift in the instantaneous frequency of the pulse that introduces the observed small error in the BFS. In fact, we made estimative calculations using the typical parameter of nonlinear coefficient for SMF that agree well with the observed frequency shift in BFS. These small residual error in the BFS can be avoided simply by making sure that we use a flat-top pulse, which can be achieved, for instance, by using a EDFA prepared for pulsed or burst operation [14].

Finally, Fig. 8 shows the BFS measurement uncertainty along the fiber calculated as the standard deviation of 5 consecutive measurements. It can be seen that the maximum uncertainty is around 1 MHz. Furthermore, as it was expected, the measurement precision and the spectra amplitude in Fig. 3(b) are directly related. The areas with larger uncertainty coincide with lower spectra amplitude. All these measurements have been performed with 1500 averages of the traces.

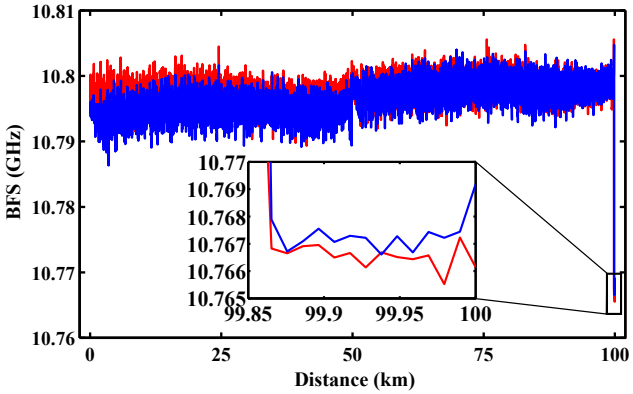

Fig. 7. Measured BFS distribution along the fiber with the pump pulses injected by the fiber's end were the hotspot is located (red line) or by the opposite end (blue line) and detail of BFS measurement in the hotspot (inset)

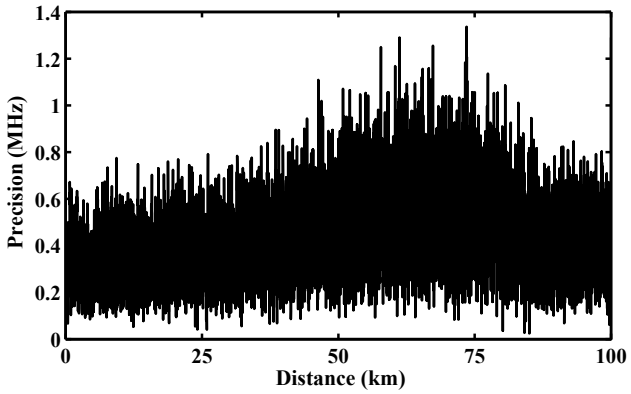

Fig. 8. Precision of the BFS measurement obtained along the fiber.

#260529
Received 4 Mar 2016; revised 2 May 2016; accepted 4 May 2016; published 1 Jun 2016

5. Conclusions

In summary, we have demonstrated a BOTDA sensor that with minor alterations to the conventional setup is able to provide gain to the pump pulses and extend the measurement range up to 100 km with 1-m resolution and 1-MHz BFS precision. This is done without the need to add any amplification scheme, such as Raman amplification, but just taking advantage of the interaction of the two waves, pump pulse and probe, that are used in all BOTDA sensors.

Acknowledgments

The authors wish to acknowledge the financial support from the Spanish Ministerio de Economía y Competitividad through project TEC2013-47264-C2-2-R, FEDER funds and the Universidad Pública de Navarra.

#260529 Received 4 Mar 2016; revised 2 May 2016; accepted 4 May 2016; published 1 Jun 2016